Journal of Physics D: Applied Physics

PAPER

Effective reduction of the coercivity for $Co_{72}Pt_{28}$ thin film by exchange coupled $Co_{81}Ir_{19}$ soft layer with negative magnetocrystalline anisotropy

To cite this article: J Y Jiao *et al* 2018 *J. Phys. D: Appl. Phys.* **51** 055007

IOP Publishing
Journal of Physics D: Applied Physics
J. Phys. D: Appl. Phys. **51** (2018) 055007 (7pp)
https://doi.org/10.1088/1361-6463/aaa389

Effective reduction of the coercivity for $Co_{72}Pt_{28}$ thin film by exchange coupled $Co_{81}Ir_{19}$ soft layer with negative magnetocrystalline anisotropy

J Y Jiao, T Y Ma, Z W Li, L Qiao, Y Wang, T Wang and F S Li

Institute of Applied Magnetics, Key Lab for Magnetism and Magnetic Materials of the Ministry of Education, Lanzhou University, Lanzhou 730000, People's Republic of China

E-mail: zweili@lzu.edu.cn and wtao@lzu.edu.cn

Received 15 September 2017, revised 6 December 2017
Accepted for publication 21 December 2017
Published 16 January 2018

Abstract

We report on the investigation of coercivity changes of the $Co_{72}Pt_{28}/Co_{81}Ir_{19}$ exchange-coupled composite (ECC) media with negative soft-layer (SL) magnetocrystalline anisotropy (MA). Our results show that the hard-layer (HL) of our sample exhibits a columnar type microstructure with well isolated grains and the SL with hcp-structure grows on top of the HL with the same texture. Therefore, strong coupling of the two layers have been realized as evidenced by the magnetic characterization. Importantly, we observe a more effective reduction of the coercivity of the ECC media by using SLs with negative MA when compared to the use of SLs with positive or negligible MA. The experimental results are corroborated by theoretical calculations.

Keywords: perpendicular magnetic recording, writability, negative magnetocrystalline anisotropy, CoPt/CoIr film

S Supplementary material for this article is available online

(Some figures may appear in colour only in the online journal)

1. Introduction

In order to solve the so called 'magentic recording trilemma' problem, different approaches, such as exchange-coupled composite (ECC) media [1–4] and heat/microwave/light assisted magnetic recording [5–7], have been used to reduce the coercivity of the recording media with very high uniaxial anisotropy constant. Among them, the ECC media, in the form of magnetically hard/soft multi-layer structure, have attracted much attention due to their promising potential in resolving the above mentioned trilemma challenge [1–4]. Extensive theoretical work has been performed to investigate the effects of soft-layer (SL) thickness [8, 9], anisotropy constant [10–12], hard-to-soft layer coupling strength [3, 13–15], and the magnetization reversal process [14, 16, 17]. Experimentally, many works have been realized with FePt [18–23], CoPt [24–28] due to their high uniaxial magnetocrystalline anisotropy (MA) which is essential to maintain high thermal stability in high density magnetic recoding. A considerable reduction of the coercivity was achieved by changing the SL composition [21, 24, 25] which alters its anisotropy constant, and by changing the SL and/or interlayer thickness [18–20, 26–28] which optimizes the hard-to-soft layer coupling strength, thus improving the writability of the media while keeping high thermal stability.

However, all of these experimental works were done with positive or negligible SL MA, K_s, in accordance with the theoretical work of Suess *et al* [11]. From the work of Suess *et al*, optimal reduction of the switching field can be realized with small but positive SL MA and the switching field will increase by increasing the anisotropy constant or by decreasing it towards the negative direction (see figure 2 in

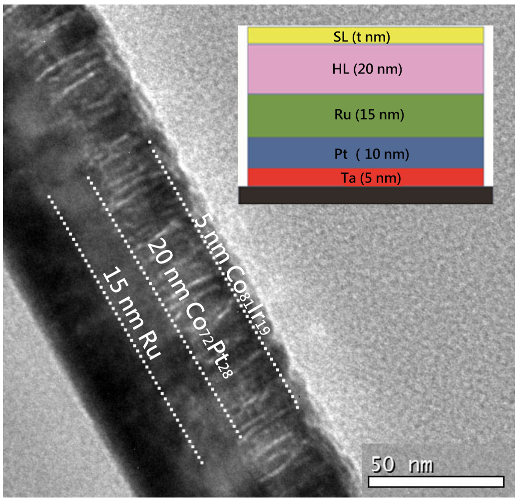

Figure 1. TEM image of the cross section of the HL/SL19 sample with the SL thickness of 5 nm. Inset shows the schematic layer structure.

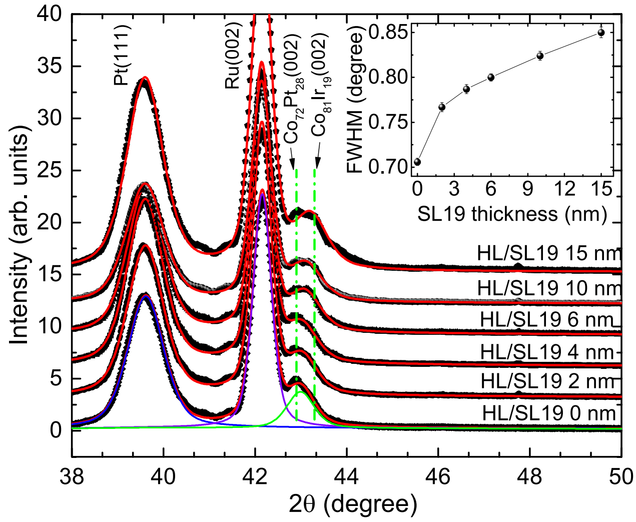

Figure 2. XRD patterns of the HL/SL19 samples with indicated soft layer thicknesses. The solid lines represent profile fitting as described in the text. Inset shows the soft layer thickness dependence of the HL/SL19 (0 0 2) peak width.

[11]). On the other hand, using the model proposed by Victora *et al* [29], Wang *et al* [12] have shown that negative SL anisotropy actually has a beneficial contribution in decreasing the switching field. To resolve the different theoretical predictions between Suess *et al* and Victora *et al* and to further optimize the magnetic properties of the ECC media, it is very interesting to experimentally investigate how does negative SL MA affect the coercivity of the ECC system.

Therefore, we report detailed studies on the reduction of its coercivity of the $Co_{72}Pt_{28}/Co_{100-x}Ir_x$ ECC system. By changing the Ir content of the $Co_{100-x}Ir_x$ SL, its MA can be tuned [30, 31]. Here, positive MA means that the easy axis of the magnetic material is along its crystallographic c-axis and negative MA, on the other hand, means that the easy axis is within its ab-plane. Thus, by oriented-growth of the hcp-$Co_{81}Ir_{19}$ (negative MA with $x = 19$) layer with its crystallographic c-axis parallel to the normal of the film surface, its magnetic moments can be restricted strictly in-plane by its negative MA, thus providing a very strong negative total in-plane anisotropy for our ECC media [32, 33]. A series of samples with different SL thickness and composition were investigated and we will show that negative SL MA is more efficient in reducing the coercivity of the ECC media, thus our results agree with the theoretical prediction of Victora *et al* [12, 29] and open a new playground for further improvements of the magnetic properties of the ECC media for high density magnetic recording.

2. Experiments

$Co_{72}Pt_{28}/Co_{81}Ir_{19}$ ECC media system ($K_s = -6 \times 10^5$ J m^{-3} [30]) were prepared by DC perpendicular magnetron sputtering method with a layered structure of substrate/Ta(5 nm)/Pt(10 nm)/Ru(15 nm)/$Co_{72}Pt_{28}$(20 nm)/$Co_{81}Ir_{19}$(t_s nm) with $t_s = 0 \sim 15$ nm (see inset of figure 1). For simplicity, our sample will be denoted as HL/SL19 where HL/SL stands for hard-layer/soft-layer and 19 represents the Ir content. Si(1 0 0)-orientation wafer with surface oxidation were used as substrate and the Ta(5 nm)/Pt(10 nm) layer was grown to promote Ru(0 0 2) texture which induces the columnar growth of the $Co_{72}Pt_{28}$ layer with well isolated grains [34, 35]. For the growth of the HL and SL, Ar pressures of 4 Pa and 0.3 Pa were used, respectively. The base pressure before deposition was lower than 2×10^{-5} Pa. For comparison reasons, ECC media systems with different SL compositions were also prepared with a similar fashion. To be exact, SL = Fe, Co and $Co_{100-x}Ir_x$ with $x = 23$, 29 and 33 systems were prepared and these samples will be denoted as HL/(Fe,Co) and HL/SL(23,29,33), respectively. Note, that all $Co_{100-x}Ir_x$ with $x = 19$, 23, 29 and 33 samples have the same crystal structure [30, 31].

Chemical composition of our thin films have been characterized by energy dispersive spectrometer. Grain morphology of the sample was measured using a transmission electron microscope (TEM). The crystal structure of our sample was characterized by x-ray diffraction (XRD) with Cu $K_{\alpha 1}$ radiation. Characterization of the magnetic properties were done with a vibrating sample magnetometer (VSM). Dynamic magnetic properties were measured with an electron spin resonance spectrometer (ESR) to determine the intrinsic magnetocrystalline anisotropy constant and the detailed procedure can be found in our previously published works [32, 33]. These measurements were all done at room temperature and our samples were stored under vacuum when the measurements are done.

3. Results and discussion

In figure 1, we present the typical TEM image of the cross section of sample HL/SL19 with $t_s = 5$ nm. Columnar growth of the $Co_{72}Pt_{28}$ layer with well isolated grains can be seen from the image and the well isolated nature of these grains are also reflected by the tilted magnetic hysteresis loop of the HL sample as shown later in figure 3(a) [35]. The XRD pattern of our sample is shown in figure 2. All samples exhibit

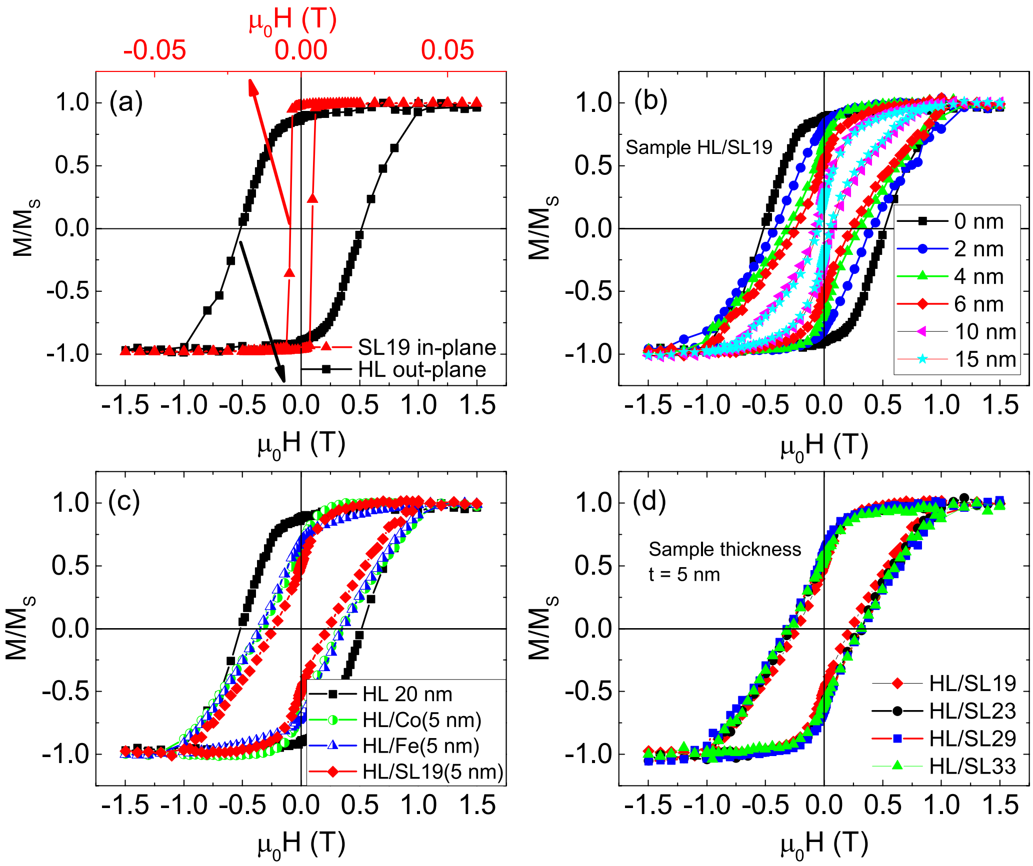

Figure 3. (a) Magnetic hysteresis loops of the separate HL and SL samples grown on the same seed-layer with applied magnetic field along the easy magnetic direction of the sample indicating good hard/soft magnetic properties. Note the very different $\mu_0 H$ scale. (b) Magnetic hysteresis loops of sample HL/SL19 with different SL thicknesses. (c) Comparison of the magnetic hysteresis loops between samples with no SL and Co(5 nm), Fe(5 nm) and SL19(5 nm) as the SL. (d) Magnetic hysteresis loops of samples HL/SL(19–33) with various SL anisotropy constant. Note that the hysteresis loops in (c) and (d) have been measured with the external field applied perpendicular to the film plane.

three main peaks at 39.6°, 42.1°, and 43.1° which correspond to Pt (1 1 1), Ru (0 0 2), and $Co_{72}Pt_{28}/Co_{81}Ir_{19}$ (0 0 2) peaks [30, 34], respectively. The minor peak at 47.7° comes from the Si substrate. A closer check on the third peak at 43.1°, one can find that the peak is actually composed of two peaks corresponding to $Co_{72}Pt_{28}$ and $Co_{81}Ir_{19}$ layers as denoted by the vertical green dash-doted lines in figure 2. However, trying to fit this peak with two sub-peaks was not successful due to their closeness and thus we fitted this peak with only one peak. The determined peak full width at half maximum (FWHM) was plotted as a function of the SL thickness, as shown in the inset of figure 2. One can see that FWHM increases with the SL thickness being consistent with the gradual increase in intensity of the SL sub-peak, inline with the gradual increase of the volume fraction of the SL. Importantly, the only observable (0 0 2) peak for the $Co_{72}Pt_{28}$ and $Co_{81}Ir_{19}$ layers indicate the oriented-growth of the these layers. Since the $Co_{72}Pt_{28}$ ($Co_{81}Ir_{19}$) layer exhibits positive (negative) MA, the easy magnetic direction of the $Co_{72}Pt_{28}$ ($Co_{81}Ir_{19}$) layer is parallel (perpendicular) to the normal of the film surface [30, 32, 34].

Normalized magnetic hysteresis loops of our sample are shown in figures 3(a)–(d). In figure 3(a), we present the measurements for $Co_{72}Pt_{28}$ and $Co_{81}Ir_{19}$ separate layers grown on the same seed-layer. The measurements were done with the applied magnetic field along the easy magnetic direction of the HL (perpendicular to the film plane) or SL (parallel to the film plane) sample. For the HL sample, the easy-axis coercivity and saturation magnetization were determined to be 0.51 T and 1.1×10^6 A m^{-1}, respectively. The MA of the HL was calculated to be 1.25×10^6 J m^{-3} by the area difference between the hard-axis and easy-axis hysteresis loops. These magnetic parameters are close to reported values of similar composition [34, 36]. The tilt of the hysteresis loop suggests a weak inter-granular coupling of the HL, which is favorable for the application in perpendicular magnetic recording [35]. For the SL sample, an easy-axis coercivity of 0.004 T and saturation magnetization of 1.2×10^6 A m^{-1} were obtained which are close to the values of our previous report [30]. These results prove that, under the current film growth conditions, HL and SL films with good structural and magnetic properties can be obtained (see the supplementary materials, available at stacks.iop.org/JPhysD/51/055007/mmedia).

In figure 3 (b), we present the measurements for our ECC sample HL/SL19 with different SL thicknesses, $t_s = 0 \sim 15$ nm. Clearly, the coercivity of the ECC system were greatly reduced. No obvious steps were observed during the magnetization reversal process, indicating strong coupling between the hard and soft layers being consistent with the absence of

Table 1. Published data on the coercivity $\mu_0 H_C$ reduction for the $Co_{100-x}Pt_x$ system using different soft layers. t_s denotes the hard/soft-layer thickness.

Hard/soft-layer	t_s (nm)	$\mu_0 H_C$ (T)	References
$CoPt$-SiO_2/Co-SiO_2	20/0–20	0.7–0.35	[26]
CoCrPt/CoTb	20/0–11	0.4–0.3	[37]
$Co_{71}Pt_{29}$-TiO_2/Co-TiO_2	15/0–15	0.47–0.2	[27]
$Co_{71}Pt_{29}$-TiO_2/$Co_{93}Pt_7$-TiO_2	15/0–15	0.47–0.3	[27]
$Co_{71}Pt_{29}$-TiO_2/$Co_{83}Pt_{17}$-TiO_2	15/0–15	0.47–0.42	[27]
$Co_{74}Pt_{22}Ni_4$/$Ni_{73}O_{27}$	12/0–20	0.75–0.3	[28]
$Co_{72}Pt_{28}$/$Co_{81}Ir_{19}$	20/0–15	0.52–0.052	[a]

[a] Indicates the current work.

any interlayers between the two layers, which shows the uniform switching of the SL with respect to the HL. However, as the SL thickness t_s increases, the perpendicular magnetic anisotropy of the ECC media is significantly degraded as the rectangular loops tend to tilt more and more with increasing t_s. This corresponds to a reduction of the squareness ratio of the hysteresis loops, which indicates the domination of the negative anisotropy of the SL, resulting in a reduction of the remanence of hysteresis loops [25].

For comparison, we also prepared HL/Co(5 nm) and HL/Fe(5 nm) ECC samples with small but positive SL MA and their magnetic hysteresis loops are shown together with that of HL/SL19(5 nm) in figure 3(c). Obviously, the SL19 layer with negative MA is more efficient in reducing the coercivity of the ECC system. Additionally, to study how the reduction of the coercivity depends on the strength of the anisotropy constant of the SL for the ECC media, we prepared different samples with different Ir content in the SL, thus different SL MA [30, 31], as shown in figure 3(d). One can see that the strength of the anisotropy constant does not have significant impacts on the media coercivity as the SL thickness does.

To see the coercivity reduction more clearly, we summarized our results in table 1 and figure 4 together with published data on the CoPt system with different SLs. Obviously, as shown in figure 4(a), $Co_{81}Ir_{19}$ SL with negative MA is more effective in reducing the ECC media coercivity for any defined SL thickness. In figure 4(b), we present the reduction of the media coercivity as a function of the SL MA constant. The data have been normalized to the value of the most right side data point at $K_s = -3.5 \times 10^5$ J m^{-3} for better comparison with calculations. The enhanced reduction with decreasing K_s is inconsistent with the predictions by Suess *et al* [11]; however is in agreement with the results of Victora *et al* [12, 29].

To understand these results more clearly, we would like to revisit the theoretical model used by Suess *et al* and Wang *et al*. In the work of Suess *et al* [11], they calculated the switching field with a simple expression $H_s = \max(H_p, H_n)$ with

$$H_n = \frac{2K_s}{\mu_0 M_1} + \frac{2A\pi^2}{4t_s^2 \mu_0 M_1}$$
$$H_p = \frac{1}{4} \times \frac{2(K_h - K_s)}{\mu_0 M_2}, \quad (1)$$

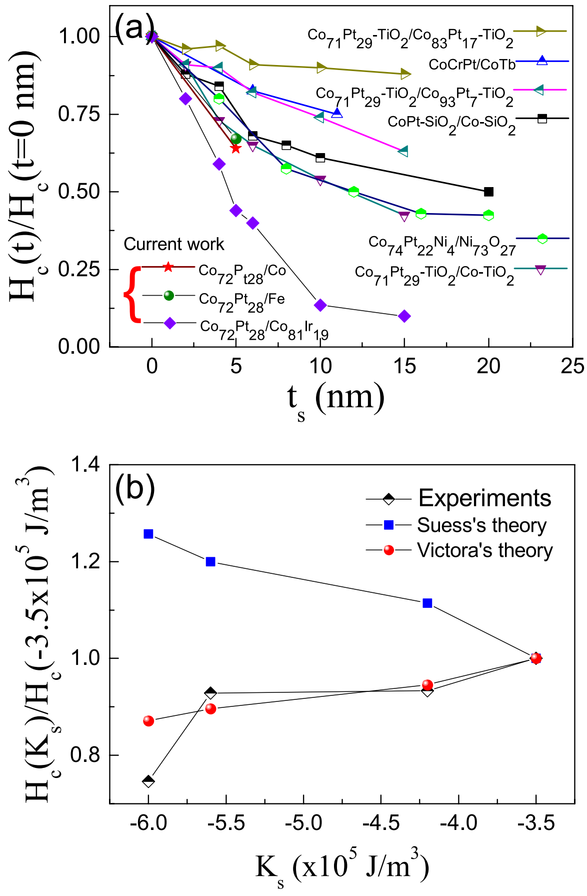

Figure 4. (a) Reduction of the coercivity of the ECC media for various HL/SL systems as a function of the SL thickness. For comparison reasons, the data were normalized to the initial value with zero SL thickness. Data with HL composition of $Co_{71}Pt_{29}$-TiO_2 was taken from [27], $CoPt$-SiO_2 was taken from [26], CoCrPt was taken from [37], and $Co_{74}Pt_{22}Ni_4$ was taken from [28]. (b) Influence of the strength of the SL MA on the coercivity of the ECC media with a SL thickness of 5 nm. Theoretical calculations were done using equation (1) (Suess's theory) and equation (2) (Victora's theory) for comparison as described in the main text.

where $\mu_0 H_n$ and $\mu_0 H_p$ represent the nucleation field in the soft layer and pinning field at the interface, respectively. K_s and K_h denote the anisotropy constants of the soft and hard layers. A is the intragranular exchange constant and M_1/M_2 is the saturation magnetization of the soft/hard layer. t_s is the soft layer thickness. On the other hand, Victora *et al* [12, 29] used a more complete model by minimizing the total energy of the ECC system. In this model, the total magnetic energy of the ECC system can be expressed by

$$E = HM_1 cos\theta_1 V_1 + HM_2 \cos\theta_2 V_2 + K_1 \sin^2\theta_1 V_1 + K_2 \sin^2\theta_2 V_2 - J_e \cos(\theta_1 - \theta_2), \quad (2)$$

where $\mu_0 H$, M_i, K_i, and V_i denote the external field, saturation magnetization, anisotropy constant and volume of the particle, respectively. Sub-index 1, 2 indicate the soft, hard region, respectively. J_e is the exchange constant and θ_i indicates the angle between the magnetic moments and the external filed. In addition, demagnetizing energy was included properly in

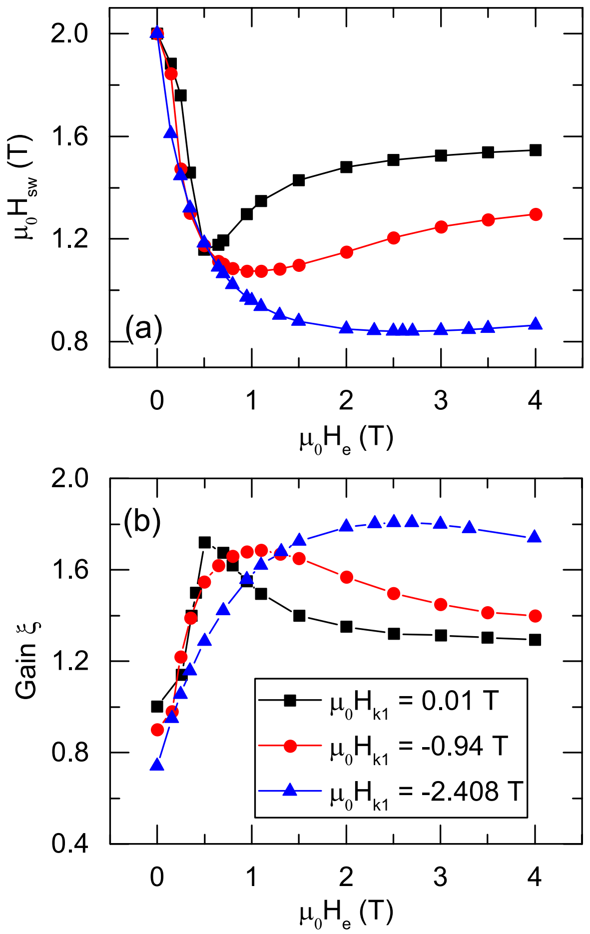

Figure 5. (a) Switching field H_{sw} as a function of the interlayer exchange field H_e with various soft layer anisotropy H_{k1}. (b) Dependence of the gain factor ξ on H_e with various H_{k1}.

this model, which was omitted by Suess *et al* in their calculation [11].

In the calculation work of Wang *et al*, Victora's model was used and the negative SL anisotropy was assumed to come from the demagnetizing field which is limited by the largest demagnetizing factor ($N = 1$) by setting the MA to zero [12]. Here, we further push the total SL anisotropy towards the negative direction by using $Co_{1-x}Ir_x$ with negative MA (total in-plane anisotropy field can be expressed as $H_{k1} = -M_s + 2K_s/\mu_0 M_s$). As shown in figure 5, we recalculated the switching field $\mu_0 H_{sw}$ and Gain factor ξ as a function of the interlayer exchange field $\mu_0 H_e$ using the same procedure as done by Wang *et al* [12] with the total in-plane anisotropy field $\mu_0 H_{k1}$ up to a negative value of -2.408 T. The gain factor, which is a reflection of the thermal stability, is defined as $\xi = 2\Delta E/(H_{sw} M_a V)$, where ΔE, M_a and V are the total anisotropy energy, average saturation magnetization, and total volume, respectively. From figures 5(a) and (b), one can see that in the strong coupling regime (bigger $\mu_0 H_e$), the more negative the SL MA, the more efficient it is in reducing the switching field and the bigger the gain factor that can be obtained. According to these results, the same conclusion can be drawn as in [12], that is, using a SL with negative K_s can further reduce the switching field of the ECC system and can further increase the gain factor ξ even up to very large negative values of the MA ($K_s = -6 \times 10^5$ J m^{-3} in our case).

In order to reproduce the same trend of our experimental results, we calculated the SL MA dependence of the coercivity reduction using the above two theories as shown in figure 4(b). Clearly, opposite to the results of Suess *et al*, Victora's theory predicts the same trend with our experiments. For the calculation, $A = 10^{-11}$ J m^{-3} and exchange field of $\mu_0 H_e = 4$ T were used. The SL thickness was set to be 5 nm which is the same as our experiments, the anisotropy constant and the saturation magnetization of the HL and SL were taken from the measured values in this work. First, calculations of the switching field were done separately using equation (1) [11] and equation (2) [12]. Then, they were normalized together with experimental data at the most right point ($K_s = -3.5 \times 10^5$ J m^{-3}) for comparison of the trends with changing MA. As shown by equation (2), Victora's model starts from a more general way and the switching field can be calculated by minimizing the total energy against θ_1 and θ_2 [12, 29]. The magnetostatic field coming from other grains of the media is considered as external field. Most importantly, it points out that the demagnetizing energy is not a negligible factor for the ECC media since it has an obvious contribution to the anisotropy of the SL. We further notice that Suess's model predicts an decrease of the thermal stability of the recording media with negative magnetocrystalline anisotropy of the SL [11]. On the other hand, in our calculation using Victora's model, we can get enhanced thermal stability for stronger inter-layer coupling regimes (larger gain factor in our calculation as discussed above.).

To check the thermal stability of our ECC media, we measured the remnant coercivity $\mu_0 H_r$ as a function of waiting time to study the magnetic decay of our sample. First, a negative saturation field of 2 T was applied, then the field was increased to positive fields around the coercive field for some waiting time t, after that the field was set to zero and measure the magnetic moment of the film. The remnant coercivity $\mu_0 H_r(t)$ can be obtained by linear fitting of the measured M(H) curve for each waiting time t. The thermal stability factor $K_u V/k_B T$ can then be evaluated by analyzing the time dependent $\mu_0 H_r(t)$ using Sharrock's equation [38],

$$Hr(t) = H_r(0)\{1 - [\frac{k_B T}{K_u V}\ln(\frac{f_0 t}{\ln 2})]^{1/n}\}, \quad (3)$$

where f_0 is called the attempt frequency ($\sim 10^{10}$ Hz for magnetic systems [38]), $n = 1.5$ was fixed [39]. $K_u V$ is the energy barrier at zero applied field, and $k_B T$ is the thermal energy required to flip the magnetization. The obtained $K_u V/k_B T$ are shown in figure 6 together with the coercivity reduction of our HL/SL19 sample. As can be seen, different with the monotonic decrease behavior of the coercivity, the thermal stability factor first increase with the SL thickness up to 6 nm and then decrease with further increase of the SL thickness. Similar to the FePt–C/FePt [4] system, the initial increase can be attributed to the increase of the switching volume due to the strong exchange coupling between the HL and SL, and the decrease above 6 nm is mainly due to the demagnetizing effect. Typical $K_u V/k_B T$ for the current perpendicular

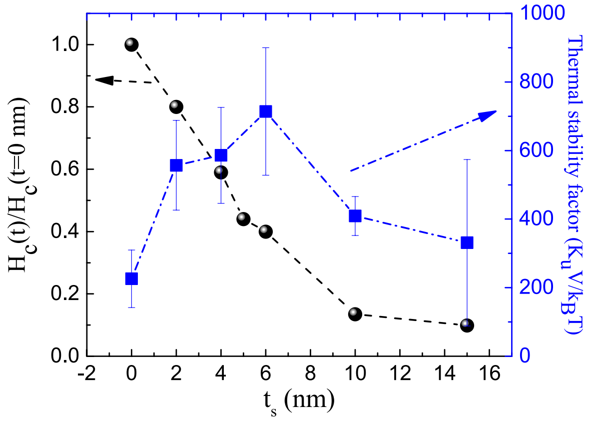

Figure 6. Thickness dependence of the normalized coercivity (left axis) and thermal stability factor (right axis) of our sample HL/SL19.

recording media using CoCrPt system is around 80 [40], which is much smaller than our value of 226 at zero SL thickness. Therefore, our ECC media show very good thermal stability and writability than the current CoCrPt perpendicular media. Finally, we would like to emphasize the advantage of Victora's model in the study of ECC media systems and the rather regretful fact that no experimental work using SLs with negative MA have been employed to reduce the coercivity of the ECC media. We hope that our work will promote further experimental work in this direction and promote further improvements of the writability for high density magnetic recording.

4. Summary

In conclusion, we have prepared $Co_{72}Pt_{28}/Co_{81}Ir_{19}$ ECC media with negative SL MA. TEM image shows the columnar growth of the $Co_{72}Pt_{28}$ HL and XRD measurements shows the oriented-growth of the SL on top of the HL with hcp-structure. Good hard/soft magnetic properties of the hard/soft layers have been proved by our VSM measurements. We observe a single step magnetization reversal of the ECC media, suggesting strong coupling of the hard and soft magnetic layers. More interestingly, we observe an enhanced reduction of the coercivity of the ECC media by using SLs with negative MA when compared to the use of SLs with small but positive MA. These results have been qualitatively reproduced by theoretical calculations. Therefore, our results provide a new direction for us to further improve the writability of the ECC media for future high density magnetic recording.

Acknowledgments

This work was supported by the National Natural Science Foundations of China (Nos. 11574122 and 11204115) and the Fundamental Research Funds for the Central Universities (Nos. lzujbky-2017-k20 and lzujbky-2017-31).

ORCID iDs

Z W Li https://orcid.org/0000-0003-2239-2802
L Qiao https://orcid.org/0000-0002-7646-3365

References

[1] Suess D, Schrefl T, Fähler S, Kirschner M, Hrkac G, Dorfbauer F and Fidler J 2005 *Appl. Phys. Lett.* **87** 012504
[2] Suess D 2006 *Appl. Phys. Lett.* **89** 113105
[3] Victora R H and Shen X 2008 *Proc. IEEE* **96** 1799–809
[4] Wang J, Sepehri-Amin H, Takahashi Y, Okamoto S, Kasai S, Kim J, Schrefl T and Hono K 2016 *Acta Mater.* **111** 47–55
[5] Varaprasad B S D C S, Chen M, Takahashi Y K and Hono K 2013 *IEEE Trans. Magn.* **49** 718–22
[6] Lu L, Wu M, Mallary M, Bertero G, Srinivasan K, Acharya R, Schultheiß H and Hoffmann A 2013 *Appl. Phys. Lett.* **103** 042413
[7] Takahashi Y K, Medapalli R, Kasai S, Wang J, Ishioka K, Wee S H, Hellwig O, Hono K and Fullerton E E 2016 *Phys. Rev. Appl.* **6** 054004
[8] Suess D, Schrefl T, Dittrich R, Kirschner M, Dorfbauer F, Hrkac G and Fidler J 2005 *J. Magn. Magn. Mater.* **290–1** 551–4
[9] Berger A, Supper N, Ikeda Y, Lengsfield B, Moser A and Fullerton E 2008 *Appl. Phys. Lett.* **93** 122502
[10] Dobin A Y and Richter H 2006 *Appl. Phys. Lett.* **89** 062512
[11] Suess D, Lee J, Fidler J and Schrefl T 2009 *J. Magn. Magn. Mater.* **321** 545–54
[12] Wang Y, Li F S, Ariake J, Honda N, Ishio S and Ouchi K 2008 *J. Magn. Magn. Mater.* **320** 3083–7
[13] Si W, Zhao G, Ran N, Peng Y, Morvan F and Wan X 2015 *Sci. Rep.* **5** 16212
[14] Richter H and Dobin A Y 2006 *J. Appl. Phys.* **99** 08Q905
[15] Ghidini M, Asti G, Pellicelli R, Pernechele C and Solzi M 2007 *J. Magn. Magn. Mater.* **316** 159–65
[16] Livshitz B, Inomata A, Neal Bertram H and Lomakin V 2007 *Appl. Phys. Lett.* **91** 182502
[17] Mukherjee S and Berger L 2006 *J. Appl. Phys.* **99** 08Q909
[18] Sun C J, Stafford D and Acharya R 2010 *IEEE Trans. Magn.* **46** 1795–7
[19] Wang F, Xu X, Liang Y, Zhang J and Wu H 2009 *Appl. Phys. Lett.* **95** 022516
[20] Tsai J L, Tzeng H T and Lin G B 2010 *Appl. Phys. Lett.* **96** 032505
[21] Guo H, Liao J, Ma B, Zhang Z, Jin Q, Wang H and Wang J 2012 *Appl. Phys. Lett.* **100** 142406
[22] Xu Z, Zhou S, Ge J, Du J and Sun L 2009 *J. Appl. Phys.* **105** 123903
[23] Guo H H, Liao J L, Ma B, Zhang Z Z, Jin Q Y, Rui W B, Du J, Wang H and Wang J P 2012 *J. Appl. Phys.* **111** 103916
[24] Pandey K, Chen J, Chow G and Hu J 2009 *Appl. Phys. Lett.* **94** 232502
[25] Saravanan P, Hsu J H, Tsai C, Tsai C, Lin Y, Kuo C, Wu J C and Lee C M 2014 *J. Appl. Phys.* **115** 243905
[26] Pandey K, Chen J, Chow G, Hu J and Lim B 2009 *J. Appl. Phys.* **105** 07B733
[27] Tang R, Chua S, Zhang W and Li Y 2011 *J. Magn. Magn. Mater.* **323** 2569–74
[28] Girt E, Dobin A Y, Valcu B, Richter H, Wu X and Nolan T P 2007 *IEEE Trans. Magn.* **43** 2166–8
[29] Victora R H and Shen X 2005 *IEEE Trans. Magn.* **41** 537–42
[30] Jiao J, Wang T, Ma T, Wang Y and Li F 2017 *Nanoscale Res. Lett.* **12** 21
[31] Hashimoto A, Saito S and Takahashi M 2006 *J. Appl. Phys.* **99** 08Q907

[32] Xu F, Wang T, Ma T, Wang Y, Zhu S and Li F 2016 *Sci. Rep.* **6** 20140
[33] Ma T, Jiao J, Li Z, Qiao L, Wang T and Li F 2017 *J. Magn. Magn. Mater.* **444** 119–24
[34] Pandey K, Chen J, Lim B and Chow G 2008 *J. Appl. Phys.* **104** 073904
[35] Mukai R, Uzumaki T and Tanaka A 2006 *IEEE Int. Magnetics Conf.* p 12
[36] Mani Pandey K, Chen J and Chow G 2006 *J. Appl. Phys.* **100** 054909
[37] Uwazumi H, Shimatsu T, Sakai Y, Enomoto K, Takenoiri S, Watanabe S, Muraoka H and Nakamura Y 2002 *J. Appl. Phys.* **91** 8058–60
[38] Sharrock M P 1994 *J. Appl. Phys.* **76** 6413–8
[39] Suess D *et al* 2007 *Phys. Rev.* B **75** 174430
[40] Piramanayagam S N 2007 *J. Appl. Phys.* **102** 011301